



ELSEVIER

Journal of Nuclear Materials 283–287 (2000) 1267–1271

Journal of
nuclear
materials

www.elsevier.nl/locate/jnucmat

Magnetic field effect on deposition of corrosion products in liquid Pb–17Li

F. Barbier *

CEA-CEREM/SCECF, CE Saclay 91191 Gif-sur-Yvette cedex, France

Abstract

This paper reports deposition data of tests carried out on Pb–17Li filled steel tubes (austenitic and martensitic) under a thermal gradient (500–250°C) and with and without a magnetic field (0.25 T). For the austenitic steel, deposits composed of nickel, manganese and tin were found at temperatures below 370°C. For higher temperatures, crystals mainly composed of iron and chromium were identified. No significant difference was observed for the test performed in a magnetic field. For the martensitic steel, various types of crystals were detected, composed of Fe and Cr or a mixture of Fe, Cr, Ni, Mn and Sn. They were found in various quantities and distributed all over the wall of the tube. A marked difference was observed in the presence of a magnetic field with a near absence of crystals in the region above the magnet. The majority of the deposits were observed in the region of the magnetic field and were composed of ferromagnetic particles of Fe and Cr (92Fe–8Cr), clearly showing a trapping effect of Fe and Cr from Pb–17Li. © 2000 Elsevier Science B.V. All rights reserved.

1. Introduction

In the water-cooled blanket concept designed for fusion reactors, the liquid Pb–17Li alloy has been proposed as tritium breeder. Previous studies have demonstrated the corrosion susceptibility of steel structural materials in this environment [1]. The corrosion products dissolved in the molten alloy and transported with the flow can be preferentially deposited in regions of low temperatures or in regions affected by the magnetic field used for plasma confinement [2]. Attention has to be given to deposition processes for the safe operation of fusion reactors. In order to remove metallic species from the liquid alloy, purification methods have to be developed. One way is to promote the formation of deposits in controlled areas either by cold trapping or by magnetic trapping. The knowledge of the deposition behavior in Pb–17Li is thus essential. This paper presents deposition data for austenitic and martensitic steels exposed to Pb–17Li

under thermal gradients and the presence of a magnetic field. It describes the nature of deposits for both steels as a function of the magnetic field and compares the results.

2. Experimental procedure

Austenitic stainless steel (type 316L: 66.7Fe–16.6Cr–11.8Ni–3.1Mo–1.8Mn) and martensitic steel (type 56T5: 86.7Fe–10.5Cr–0.66Ni–0.65Mo–0.61Mn–0.48Nb–0.18V–0.22Si) were used as materials. They were used as tubes (Fig. 1) which were closed at one end by welding, filled with liquid Pb–17Li under an argon atmosphere and finally sealed under vacuum.

For each steel exposed to Pb–17Li, two tubes were prepared: one was placed under thermal gradient without a magnetic field, the second one was placed under a similar thermal gradient and under a magnetic field. All tubes were mounted vertically in a furnace where the temperature gradient was established for the test duration. The gradient was obtained such that the hot end of the tube was at the top in order to minimize thermal convection. The temperature was measured at

* Tel.: +33-1 69 08 16 13; fax: +33-1 69 08 15 86.

E-mail address: barbier@ortolan.cea.fr (F. Barbier).

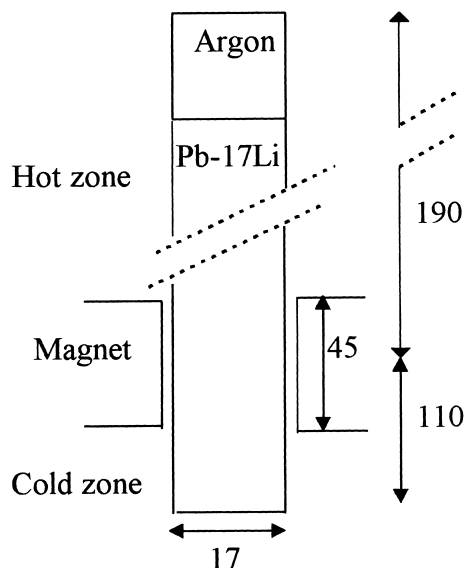


Fig. 1. Schematic drawing of a steel tube exposed to Pb-17Li (dimensions are given in mm).

centimeter intervals along the tubes, using thermocouples fixed to external surface of the tube. The isothermal hot zone was about 5 cm in length whereas the non-isothermal zone exhibited a temperature change of about 10°C per cm, yielding a temperature gradient of 510–250°C.

For those tests with a magnetic field, a similar temperature gradient was established and a permanent magnet (0.25 T) was placed 190 mm below the top of the tube in a temperature region ranging from 390°C to 320°C (Fig. 1). On completion of tests (3300 h), the heating was stopped and the tubes were cooled in ambient air.

After cooling, the tubes were sectioned longitudinally in order to obtain a quarter and a three quarters of the tube. The latter one was cut in several slices (perpendicular to the tube axis) which were polished. In this manner, the cross-section of the steel/Pb-17Li interface was available for observation. The remainder of the tube was used for direct observation of deposits on the wall after removal of Pb-17Li in a chemical mixture of acetic acid, hydrogen peroxide and ethanol mixture (1:1:1). This solution was filtered and analyzed by atomic absorption spectroscopy to determine the concentration of metallic elements remaining in Pb-17Li at the end of the corrosion/deposition test.

The walls of tubes (cut into 5 cm lengths) and the polished samples were examined by scanning electron microscopy (SEM) and compositional information (given in wt%) was obtained by energy dispersive X-ray analysis (EDX).

3. Results and discussion

3.1. Austenitic steel

3.1.1. Deposition without magnetic field

The surface of the 316L steel exposed to Pb-17Li exhibited a ferritic corrosion layer as expected from literature [1]. The formation of this layer depleted in nickel indicates a large mass transfer of this element in Pb-17Li but other elements as Fe, Mn and Cr were also transported, in agreement with the observed deposits.

Two distinct categories of deposits were found. In the temperature range 370–350°C, many crystals were observed adhering to the wall of the tube and in the frozen alloy (Fig. 2). They were also identified at lower temperatures but they were less abundant. Their average composition was (36–40)Ni–(25–18)Mn–(35–46)Sn, corresponding to the ternary compound Ni₂MnSn [3]. Other crystals of composition (54–50)Ni–(46–50)Mn were also found, corresponding to the binary compound NiMn [4]. The formation of the ternary crystals Ni–Mn–Sn is not simple to explain as Pb-17Li and steel contained very low tin concentration (6 and 36 wppm, respectively). Nevertheless, such compounds were already detected in previous works [5–7]. In fact, there exists a strong interaction between Ni and Mn [8], which explains why nickel and manganese are never deposited as single elements but always associated. The observation of Ni–Mn–Sn crystals indicates that tin also interacts preferentially with nickel and manganese.

In regions which had been at temperatures ranging from 500°C to 400°C, deposits mainly composed of iron and chromium were found. Fe-rich crystals (87Fe–11Cr–1Ni–1Mn) were observed in the hottest zone (Fig. 3). For temperatures around 480°C, crystals of composition 56Fe–44Cr were also detected. In the temperature range 480–450°C, analysis indicated Cr-rich crystals (30Fe–70Cr). Therefore, there is a temperature effect on composition with a change from iron-rich to

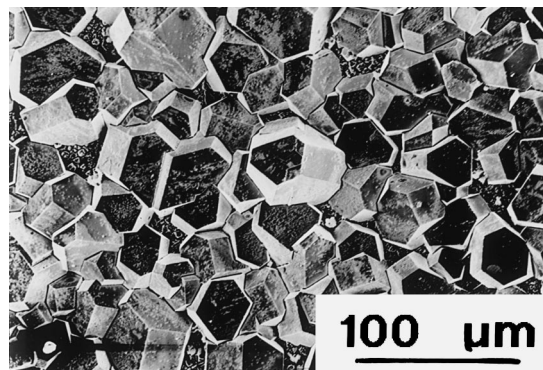


Fig. 2. SEM micrograph showing Ni₂MnSn crystals.

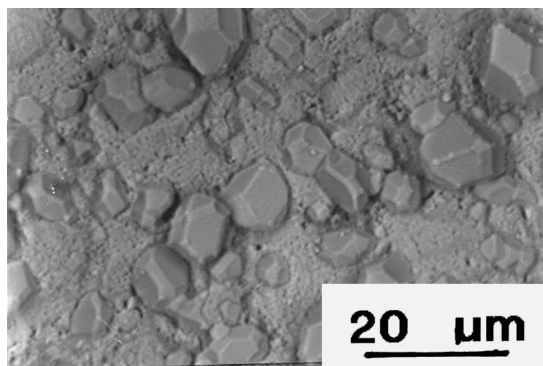


Fig. 3. SEM micrograph showing Fe-rich crystals.

chromium-rich with decreasing temperature. These observations are in agreement with those reported in literature [9–11].

3.1.2. Deposition with magnetic field

The two types of deposits described above were also found in the test incorporating a magnetic field. As with the previous tests, Ni_2MnSn and NiMn crystals were detected in the temperature zone less than 400°C . This deposit seemed unaffected by the presence of the magnetic field. Crystals composed of Fe and Cr were observed in the zone corresponding to the temperature range $500\text{--}400^\circ\text{C}$. In fact, in the zone surrounded by the magnet ($390\text{--}320^\circ\text{C}$), no clear effect of the field was found. The only evidence for a magnetic field effect was the presence of a few Cr-rich crystals ($22\text{Fe}\text{--}5\text{Ni}\text{--}73\text{Cr}$) on one side of the tube at about 360°C . As reported in Section 3.1.1, such crystals were found at higher temperatures in the test without a magnetic field. However, this result is not significant enough to draw any conclusions. In the same way, for both tests, analysis of solutions used to dissolve $\text{Pb}\text{--}17\text{Li}$ did not indicate any differences in Fe and Cr concentrations. Therefore, it is difficult to conclude if a magnetic field effects deposition in type 316L systems. In a previous work [11], it was reported that the field destroys the temperature dependence on composition of Fe/Cr deposits. Our results do not show that trend but the experimental conditions are not exactly the same (e.g., the temperature gradient is different and the temperature region corresponding to the magnet location is not defined in [11]).

3.2. Martensitic steel

3.2.1. Deposition without magnetic field

No visible corrosion layer was observed on the surface of the 56T5 steel, with the evidence for corrosion being the direct observation of deposited crystals. The main constituents of this steel seem to corrode at a similar rate when it is in contact with molten $\text{Pb}\text{--}17\text{Li}$. Nevertheless,

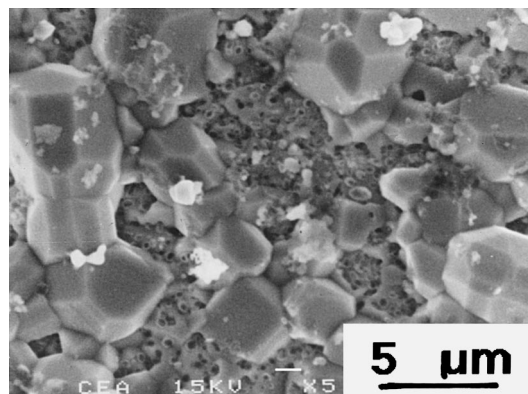


Fig. 4. SEM micrograph showing majority of Fe-rich crystals ($97.5\text{Fe}\text{--}2.5\text{Cr}$) with a few $\text{Ni}\text{--}\text{Fe}\text{--}\text{Mn}\text{--}\text{Sn}$ crystals (in white).

an increase in the surface roughness was observed and EDX analysis showed chromium depletion near the interface yielding a composition of $89.8\text{Fe}\text{--}7.8\text{Cr}\text{--}0.3\text{Ni}\text{--}0.8\text{Mo}\text{--}0.7\text{Mn}\text{--}0.6\text{Nb}$. Metallic elements were found in the solution used to dissolve $\text{Pb}\text{--}17\text{Li}$ (in wppm): 13 for Fe, 3.5 for Mn, <1.5 for Cr and <0.7 for Ni.

The characterization of crystals deposited on the steel surface was complex because they were distributed all over the wall of the tube and exhibited varying compositions. Nevertheless, some results may be drawn (Fig. 4). The hottest part of the tube ($510\text{--}480^\circ\text{C}$) was mainly composed of Fe-rich crystals having the composition $97.5\text{Fe}\text{--}2.5\text{Cr}$. In the temperature range $480\text{--}400^\circ\text{C}$, other types of crystals were observed in small quantities: Fe–Cr crystals ($38\text{Fe}\text{--}59\text{Cr}\text{--}3\text{Mo}$), $\text{Ni}\text{--}\text{Fe}\text{--}\text{Mn}\text{--}\text{Sn}$ crystals ($29.2\text{Ni}\text{--}27.2\text{Fe}\text{--}14\text{Mn}\text{--}28.3\text{Sn}\text{--}1.1\text{Cr}\text{--}0.3\text{Mo}$) and Fe–Nb crystals ($28.2\text{Fe}\text{--}65.7\text{Nb}\text{--}2.5\text{Cr}\text{--}3\text{Mo}$). For lower temperature ($T < 400^\circ\text{C}$), the $\text{Ni}\text{--}\text{Fe}\text{--}\text{Mn}\text{--}\text{Sn}$ crystals were found associated with higher chromium content ($32\text{Ni}\text{--}10.5\text{Fe}\text{--}16\text{Mn}\text{--}33.5\text{Sn}\text{--}8\text{Cr}$). It was deduced that the Fe/Cr ratio of these crystals decreases with temperature. However, at temperatures less than 350°C , the Fe and Cr concentrations were both lowered and the crystals reach the composition $33.5\text{Ni}\text{--}7\text{Fe}\text{--}18\text{Mn}\text{--}39\text{Sn}\text{--}2.5\text{Cr}$ which corresponds to the ternary compound $(\text{Ni},\text{Fe},\text{Cr})_2\text{MnSn}$. The observation of this compound in presence of small quantities of Ni, Mn and Sn confirms the strong interaction between these elements as reported in Section 3.1.1.

3.2.2. Deposition with magnetic field

The corrosion behavior of 56T5 steel is similar to that observed previously. Corrosion is detected because deposited crystals are found. The concentration of metallic elements present in $\text{Pb}\text{--}17\text{Li}$ alloy at the end of this test has been determined. It was found (in wppm): 6.5 for Fe and 1.9 for Cr. The Fe concentration is thus divided by a factor of 2 compared to test without magnetic field (Section 3.2.1).

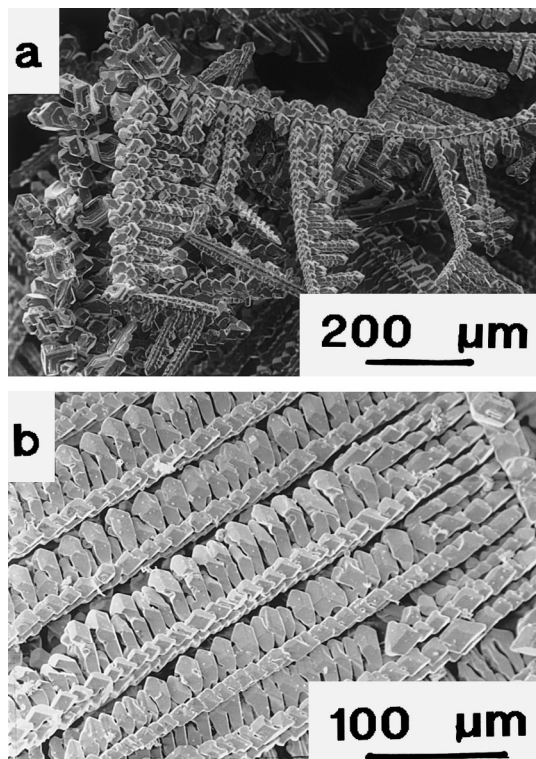


Fig. 5. SEM micrographs showing Fe–Cr crystals in the region of the tube under magnetic field: (a) general view of crystals formed in the frozen alloy, and (b) orientated 92Fe–8Cr crystals.

With regard to the distribution of crystals, the situation was completely different from that presented above. In fact, the region, which had been at a temperature ranging from 510°C to 390°C during the test, was nearly free from deposition. Most of the crystals were found in the region, which was directly in the magnetic field (temperature range 390–320°C). Fig. 5 shows the abundant crystals, which were detected, in this area after removal of Pb–17Li. Further evidence for the effect of the magnetic field is the fact that the crystals are not randomly distributed but orientated along specific directions (Fig. 5(b)). The EDX analysis indicates they are composed of iron and chromium: 92Fe–8Cr. A large quantity of these crystals was suspended in the frozen alloy (about 75 mg) but some amount was also found adhering to the surface of the tube (Fig. 6). For temperatures less than 300°C (corresponding to the region below the magnetic field), some crystals were sparsely detected. The analysis showed their composition to be a mixture of Ni, Mn and Sn corresponding to the ternary compound $(\text{Ni,Fe,Cr})_2\text{MnSn}$. The deposition of this material seems unaffected by the magnet because it was also found in a similar temperature range for the test performed without a magnetic field.

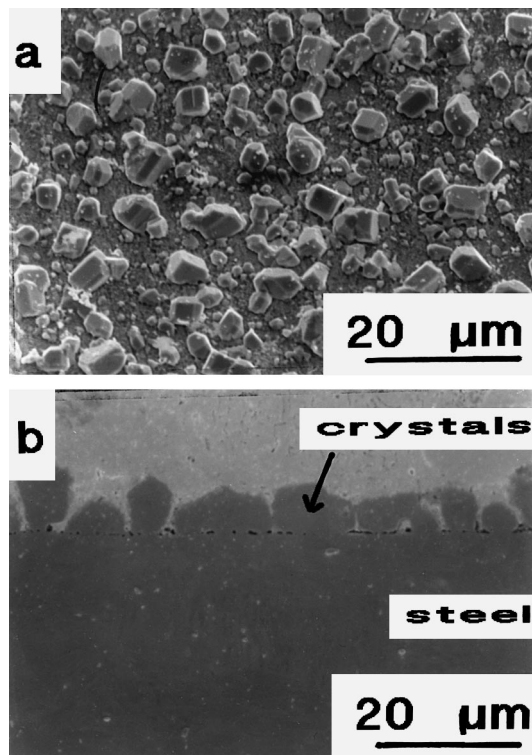


Fig. 6. SEM micrograph showing Fe–Cr crystals adhering to the surface of the tube placed in the magnet: (a) direct view, and (b) cross section.

The presence of the magnetic field significantly alters the distribution of corrosion products formed under thermal gradient in martensitic steel systems. Preferential deposition of ferromagnetic Fe–Cr crystals in the region of the field is clearly observed. The deposition behavior is well consistent with the decrease of the Fe content remaining in the Pb–17Li alloy at the end of the test, indicating magnetic trapping effect. Furthermore, different behaviors are found for both steels. This could be mainly explained by differences of compositions but also of physical properties (316L steel is non-magnetic and 56T5 steel is magnetic). The latter one could influence the magnetic field lines and thus the deposition of crystals.

4. Conclusions

A series of simple deposition tests have been carried out in liquid Pb–17Li contained in austenitic and martensitic steel tubes under a thermal gradient.

In the 316L steel systems, deposits composed of nickel, manganese and tin were found at temperatures below 370°C. In the temperature range 500–400°C, crystals mainly composed of iron and chromium were identified. They were Cr-rich at the lower temperature

and Fe-rich at the higher temperature. No significant differences were observed with the test under a magnetic field.

In the 56T5 steel systems, different types of crystals were detected. They were found in various quantities and distributed all over the wall of the tube, the Fe/Cr ratio decreasing with temperature. In presence of a magnetic field, there was a marked difference in behavior. There was nearly an absence of crystals in the high temperature region above the magnet. The majority of deposits were observed in the region placed in the magnetic field, some adhering to the wall and some suspended in Pb–17Li. Only one type of this ferromagnetic deposit composed of Fe and Cr (92Fe–8Cr) was found. The magnetic field had no effect on the small amount of deposits composed of Ni, Mn and Sn.

For martensitic steel systems, there is thus evidence for a magnetic field effect on the trapping of ferromagnetic material. Deposition is preferentially observed in the region of the field and the concentration of iron remaining in solution in Pb–17Li is lowered (purification effect). Therefore, magnetic trapping could be used to remove Fe and Cr from the liquid alloy.

Acknowledgements

This work has been supported by EC in the frame of the fusion technology programme (task action UT-

SM&C-LiPb). The author wishes to thank F. Herbert for SEM examination and practical assistance.

References

- [1] T. Flament, P. Tortorelli, V. Coen, H.U. Borgstedt, *J. Nucl. Mater.* 191–194 (1992) 132.
- [2] F. Barbier, A. Alemany, S. Martemianov, *Fus. Eng. Des.* 43 (1998) 199.
- [3] Landolt-Bornstein, Numerical data and functional relationships in science and technology, in: O. Madelung (Ed.), *Substance Index 1993*, Subvolume b, Ternary Substances, Springer, Berlin, p. 733.
- [4] N.A. Gokcen, Binary alloy phase diagrams, in: T.B. Massalski (Ed.), *ASM 3* (1991) 2580.
- [5] F. Barbier, F. Herbert, R. Terrasson, CEA Report SCECF RT 346, November 1994.
- [6] F. Barbier, B. Joseph, F. Herbert, R. Terrasson, CEA Report SCECF RT 347, November 1994.
- [7] M.G. Barker, D.J. Siddons, F. Barbier, *J. Nucl. Mater.* 233–237 (1996) 1436.
- [8] F. Barbier, *Fus. Technol.* 2 (1994) 1261.
- [9] P.F. Tortorelli, *Fus. Eng. Des.* 14 (1991) 335.
- [10] A. Terlain, T. Flament, T. Dufrenoy, J. Sannier, *J. Nucl. Mater.* 191–194 (1992) 984.
- [11] M.G. Barker, M.J. Capaldi, *J. Nucl. Mater.* 212–215 (1994) 1534.